Reaction Dynamics

DOI: 10.1002/ange.201301973

Dynamics of a Nanometer-Sized Uranyl Cluster in Solution**

Rene L. Johnson, C. André Ohlin, Kristi Pellegrini, Peter C. Burns, and William H. Casey**

The discovery of a family of large uranyl peroxo clusters[1] has dramatically affected the ideas about the environmental chemistry of actinide elements.[2] To date more than 40 structures have been isolated and have proven to make up a heterogeneous class in terms of size, structural motifs, solution stability, and speciation.[3] In spite of their likely importance as environmentally relevant species, little is known about the solution dynamics of these clusters, such as dissociation mechanisms and electrochemical stabilities. An added challenge has been the isolation of large quantities of pure compound with NMR-active nuclei in the structure.[4] Here we probe the solution chemistry of a uranyl peroxo cluster that contains 24 uranyl moieties linked by 12 pyrophosphate units. This oblong uranyl pyrophosphate cluster[5] has a nominal stoichiometry of $[(UO_2)_{24}(O_2)_{24}(HP_2O_7)_6(H_2P_2O_7)_6]^{30-}$ (Figure 1, $U_{24}P$), is soluble in aqueous solution over a wide pH range and is easily detected by ^{31}P NMR spectroscopy.

The $U_{24}P$ cluster crystallizes as $Na_{30}[(UO_2)_{24}(O_2)_{24}(HP_2O_7)_6(H_2P_2O_7)_6]\cdot n\,H_2O$ and is oblate ($e = 0.54$, see the Supporting Information).[5] The dimensions of the molecule are $1.70\text{ nm} \times 1.89\text{ nm} \times 1.99\text{ nm}$, and it contains internal sodium ions and has four unique phosphate sites in the crystal structure. These four phosphorus sites are present in a 4:4:8:8 ratio (labeled A, B, C, and D in Figure 1). The distance between the two A sites is approximately 0.3 nm longer than between the two B sites. Sites C and D differ, because they border molecular cavities of two geometries—the cavities differ in size from one another by approximately 0.6 nm, judged to be the distance between the nearest but opposite atoms. However dissolving a pure crystalline sample of $U_{24}P$ yields an NMR spectrum with two ^{31}P NMR signals in a 1:2 ratio. These two signals indicate that the chemical environments around sites A and B, and C and D, are dynamically averaged to each give rise to a single peak in solution for each pair of sites. ^{23}Na NMR spectroscopy yields a single broad peak, thereby making it impossible to distinguish between internal and external sodium ions.[5]

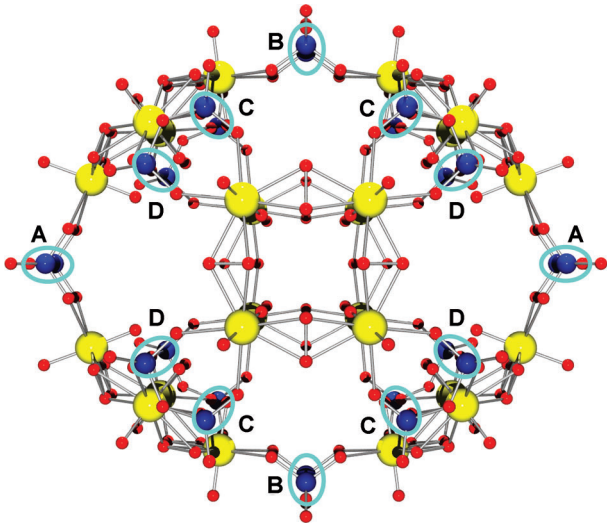

Figure 1. Inequivalent ^{31}P sites of the $U_{24}P$ cluster. O red, U yellow, P blue. The four pyrophosphate sites A–D are circled and labeled.

To establish that the two ^{31}P signals were from the same large ion, we conducted diffusion-ordered spectroscopy (DOSY) using ^{31}P NMR spectroscopy. The calculated diffusion coefficients for the two ^{31}P signals are virtually identical at $(1.64 \pm 0.05) \times 10^{-6}$ and $(1.61 \pm 0.03) \times 10^{-6}\ cm^2 s^{-1}$. When treating the molecule as a sphere, the effective hydrodynamic radius (r) of the molecule in solution is estimated from the Stokes–Einstein equation

$$D = \frac{k_B T}{6\pi\eta r} \quad (1)$$

where k_B is Boltzmann's constant, T is the temperature, and η is the viscosity of water (8.9×10^{-4} Pa s). The estimated hydrodynamic radius is (1.50 ± 0.01) nm, which is similar to, but larger than, the approximate crystallographic radius of 1.0 nm. The discrepancy is due to the presence of the solvation shell. These DOSY data in conjunction with the constant 1:2 ratio between the signals are strong evidence that the two ^{31}P signals originate from the same large molecule and that the $U_{24}P$ cluster is released intact into solution.

[*] R. L. Johnson, Prof. W. H. Casey
Department of Chemistry, University of California, Davis
1 Shields Ave, Davis, CA 95616 (USA)
E-mail: whcasey@ucdavis.edu
Dr. C. A. Ohlin
School of Chemistry, Monash University
Clayton, Victoria 3800 (Australia)
E-mail: andy.ohlin@monash.edu
K. Pellegrini, Prof. P. C. Burns
Department of Civil and Environmental Engineering and Earth Sciences, University of Notre Dame (USA)
Prof. P. C. Burns
Department of Chemistry and Biochemistry
University of Notre Dame (USA)
Prof. W. H. Casey
Department of Geology, University of California, Davis (USA)

[**] This work is supported by the Office of Basic Energy Science of the U.S. Department of Energy as part of the Materials Science of Actinides Energy Frontier Research Center (DE-SC0001089). Additional funding sources are listed in the Supporting Information.

Supporting information for this article is available on the WWW under http://dx.doi.org/10.1002/anie.201301973.

The solution chemistry of $U_{24}P$ was probed over a wide range of pH values by dissolving crystals into buffered (0.050 M) solutions. The sodium ion concentration in solution reaches 0.14 M from the counterion sodium ions alone, which we augmented with $NaNO_3$ (0.010 M). To examine the effect of other counterions, we prepared separate solutions with 0.30 M of tetramethylammonium (TMA), tetraethylammonium (TEA), or tetrabutylammonium (TBA) nitrate, which results in a final ionic strength of approximately 0.49 M (0.14 M $Na^+ + 0.30$ M tetraalkylammonium nitrate + 0.050 M buffer) if the highly charged $U_{24}P$ is excluded from the ionic-strength calculation. Attempts to synthesize the cluster with other counterions, so that a mixed solution (i.e. $Na^+ + TMA$) could be avoided, failed. Similarly, addition of other alkali counterions, including the use of $NaNO_3$ (0.30 M) as well as attempting to include 0.30 M tetrapropylammonium nitrate, caused precipitation.

At room temperature and at pH < 8 the two ^{31}P NMR signals are at 3.0 and 4.0 ppm, but they move to 3.4 and 4.2 ppm when the pH value is increased to above 8. Furthermore, these signals broaden and coalesce as the temperature increases, indicating chemical exchange (Figure 2). At the highest temperatures, the molecule dissociates, as observed by irreversible changes in the NMR spectrum, and the extent of the dissociation depends on the pH value. Below pH 9 and at elevated temperatures the molecule is more extensively degraded than at higher pH values at the same temperature (see the Supporting Information, Figure 4 for all stacked plots measured at different pH values). However, the broadening and coalescence are fully reversible and do not depend on the pH value. We further verified chemical exchange using nuclear Overhauser effect spectroscopy (NOESY; the Supporting Information, Figure 5).[6] The cross peaks confirm that the two sites are linked either by magnetization transfer or by dipole–dipole interaction, although the rigidity of the structure likely prevents the latter.

The simplest interpretation is that the $U_{24}P$ ion is in equilibrium with a more symmetric form in which all ^{31}P sites are chemically equivalent. This symmetric intermediate allows for transfer of individual phosphorus atoms between different sites without breaking any of the eight bonds per pyrophosphate unit. As a consequence, sites A, B, C, and D are all in equilibrium with one another.

To estimate rate coefficients, we fit the one-dimensional NMR data to a three-site two-molecule exchange model obtained by analytically solving the Bloch equations[7] modified by using the McConnell formalism[8] (see the Supporting Information). The rates obtained from this model become related to a simple two-site one-molecule model by a simple prefactor under conditions where the equilibrium between the spherical intermediate and the observed elliptic form of the molecule favors the aspherical ion; so this latter model can be used as well, which reduces complexity during multivariate fitting. The data from pH 9.36 are shown in Figure 3. Activation parameters were calculated by using the temperature-dependent rate coefficients and the Eyring–

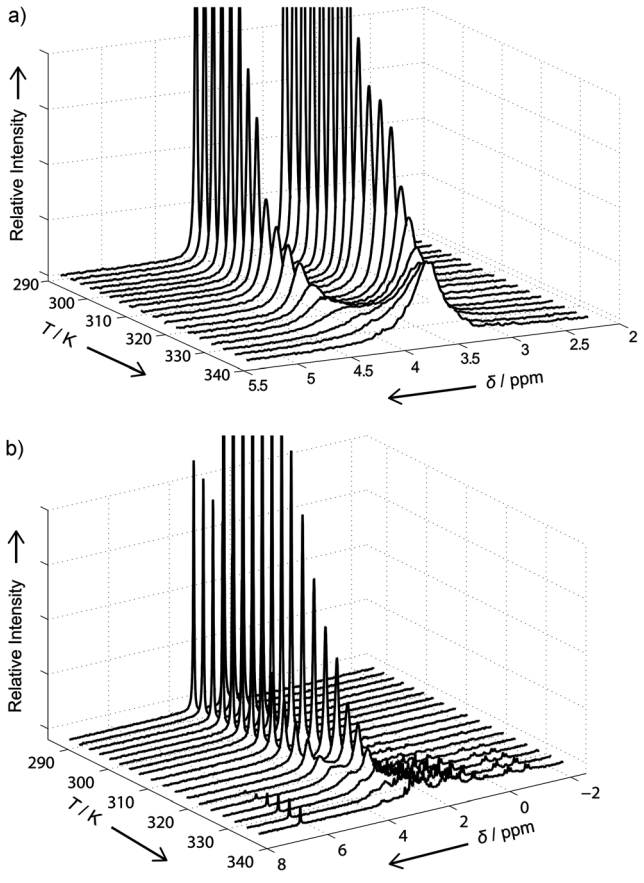

Figure 2. Stacked ^{31}P NMR spectra as a function of temperature for the $U_{24}P$ cluster at pH 9.36 (a) and at pH 7.11 (b), both of which were constant. The gradual broadening and coalescence of the two peaks indicates that the sites have become equivalent on the NMR time scale. At temperatures above coalescence, we observe dissociation of $U_{24}P$ at pH < 9 (see text).

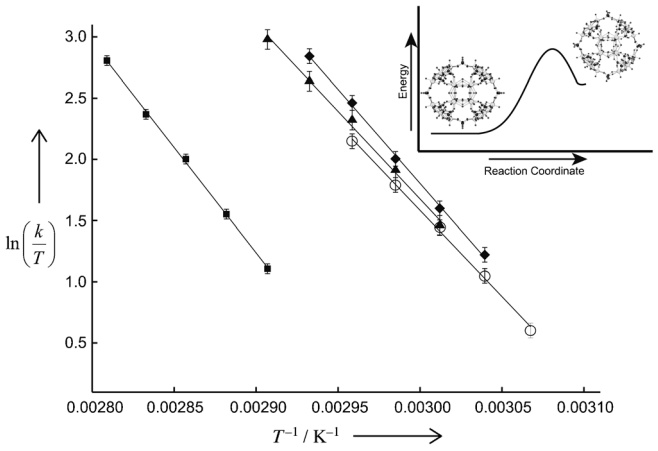

Figure 3. Eyring–Polanyi plot of the rate versus temperature. The rate data estimated from ^{31}P NMR spectra of $U_{24}P$ (0.0046 M) in 3-(cyclohexylamino)-1-propanesulfonic acid (CAPS, 0.050 M) buffer as a function of temperature. Circles (○) correspond to a solution with additional 0.010 M sodium nitrate and a final pH of 9.36; squares (■) to 0.30 M TMA nitrate, at pH 9.58; triangles (▲) to 0.30 M TEA nitrate, at pH 9.49; and diamonds (◆) to 0.30 M TBA nitrate, at pH 9.47. Error bars indicate two standard errors of the linear regression, and the inset shows our interpretation of the reaction.

Polanyi equation. For the solution with only Na^+ countercations (ca. 0.14 M), we estimate $k_{298} = (9.7 \pm 0.6)\ s^{-1}$, $\Delta H^{\neq} = (115 \pm 3)\ kJ\,mol^{-1}$, and $\Delta S^{\neq} = (163 \pm 8)\ J\,mol^{-1}K^{-1}$ with the uncertainties corresponding to two estimated standard errors of the regression.

The reaction rate coefficients are dramatically affected by the presence of the larger TMA ion (solvated radius = 3.22 Å[9]). In the solution augmented with TMA[NO_3] (ca. 0.30 M + 0.14 M Na^+), the rate coefficient decreases by almost a factor of 30, with $k_{298} = (0.40 \pm 0.02)\ s^{-1}$, $\Delta H^{\neq} = (140 \pm 2)\ kJ\,mol^{-1}$, and $\Delta S^{\neq} = (223 \pm 7)\ J\,mol^{-1}K^{-1}$ (Figure 3). Clearly, TMA ions stabilize the $U_{24}P$ structure in its oblate, charge-separated form and increase both the activation energy and activation entropy. The increased activation entropy in the presence of TMA ions suggests changes in solvation that might be detectable by using high-pressure NMR spectroscopy and establishment of an activation volume, given the large (10–18 $cm^3\,mol^{-1}$) volume change per water molecule displaced.

Although the radius of the Na^+ ion (1.02 Å[9b]) is considerably smaller, the radius of the TMA ion is still small enough to potentially allow it to move into the $U_{24}P$ cluster, which may be a key feature of how TMA ions stabilize the $U_{24}P$ structure. The radius of alkylammonium ions in solution decreases as the temperature increases,[10] which may account for why higher temperatures are necessary to cause the conformational change when TMA ions are present in solution. The larger alkylammonium counterions TEA (radius = 3.85 Å,[9] $k_{298} = (9.7 \pm 0.8)\ s^{-1}$, $\Delta H^{\neq} = (116 \pm 4)\ kJ\,mol^{-1}$, and $\Delta S^{\neq} = (170 \pm 13)\ J\,mol^{-1}K^{-1}$) and TBA (radius = 4.77 Å,[10] $k_{298} = (7.7 \pm 0.5)\ s^{-1}$, $\Delta H^{\neq} = (125 \pm 3)\ kJ\,mol^{-1}$, and $\Delta S^{\neq} = (196 \pm 8)\ J\,mol^{-1}K^{-1}$) have no such effect on the $U_{24}P$ cluster, and instead the cluster behaves as though only Na^+ counterions were present (Figure 3). The ionic strength may have an effect for all the alkylammonium samples, but the smaller size of the TMA ion can allow it to compete successfully with the Na^+ ion to stabilize the cluster, and those effects are far greater than that of ionic strength alone. TEA and TBA ions are apparently too large to stabilize the cluster in this way, so that only a slight offset in the linear Eyring–Polanyi plot of TEA and TBA is observed relative to that of Na^+ (Figure 3). These differences are larger than, but close to, the experimental error.

High-pressure measurements (see the Experimental Section) were also performed at pH 9.24 with the Na^+ countercation and CAPS buffer near the coalescence temperature (325.5 K). As pressure increased, the two signals moved further apart and became more narrow (see the Supporting Information, Figure 6). These spectral changes clearly indicate that pressure suppresses formation of the symmetric intermediate, thereby hindering transfer or scrambling of phosphorus between different sites. By calculating the pressure dependence of the rate coefficient we estimated a volume of activation of $\Delta V^{\neq} = +(11.6 \pm 0.5)\ cm^3\,mol^{-1}$. The $\Delta V^{\neq}$ value indicates pressure-induced changes in solvation that stabilize the asymmetric form, such as storage of a water molecule in the core.

Our results show that an f-block polyoxoanion fluctuates between at least two structural forms. Given that more than 40 such uranyl peroxo structures are known to date, the results from the $U_{24}P$ cluster provide key insight into the relation between molecular size, structure, and dynamics of large uranyl oxides in solution. This is the first metastable equilibrium observed for actinyl peroxo clusters, but the findings are consistent with some observations for other polyoxometalate ions. For example, five structural isomers of Keggin[11] polyoxotungstates are known, and controlled conversions between α- and β-structures have been demonstrated,[12] but these conversions required higher temperatures and longer reaction times than used in the present study. It is unknown if isolation of the hypothesized spherical species is possible, since the spherical $U_{24}P$ may be considered to be a metastable intermediate as opposed to a fully stable, isolatable structure. Protonation of the pyrophosphate groups in the $U_{24}P$ cluster help explain the pH dependence of dissociation of such clusters. The connection between the dynamic behavior of $U_{24}P$ and the counterions suggests that these will also affect dissociation.

The dynamic equilibrium we demonstrate here links to a much broader debate about general control of reactivity of oxide surfaces in water, since ions like $U_{24}P$ are of the same general size as reactive kink sites on surface steps in growing and dissolving minerals. The reactivity of oxide surfaces of minerals in water are traditionally explained by invoking transition states of a few atoms at the surface,[13] or by using step-flow models[14] that emphasize microscopic step geometries and the Gibbs–Thomson energetics. Neither approach is satisfying, the first because the transition states may be irrelevant and the second because the models are inherently at the supermolecular scale. The alternative[15] argues that rates of oxygen-isotope exchanges and dissociation reactions proceed via low-energy metastable states similar to those documented[16] in polyoxometalate ions. Such metastable structures form through concerted movements of many atoms at nanometer-sized steps to establish an equilibrium, and often this process involves separation of charges in solution, which explains why even nominally inert counterions influence the rates of reaction, as we show here.[17] Our observations provide strong evidence for the importance and reality of such metastable intermediates.

Experimental Section

Crystals of $Na_{30}[(UO_2)_{24}(O_2)_{24}(HP_2O_7)_6(H_2P_2O_7)_{12}]\cdot n\,H_2O$ were synthesized according to a modified version of a published method (the Supporting Information, Table 2).[7] Crystals were hand-picked from the mother liquor, rinsed with deionized (DI) water, and dried on a filter. Samples for NMR spectroscopy were prepared immediately prior to analysis. All samples contained $U_{24}P$ (4.6 mM) in buffer (0.050 M), and electrolyte (see the Supporting Information, Table 3 for the pH values and buffer list. Solutions (250 μL) were placed in a polytetrafluoroethylene (PTFE) NMR tube insert before being placed in standard 5 mm NMR borosilicate tubes with about 105 μL of $NaNO_3$ (0.010 M); for experiments with TMA, TEA, and TBA ions no solution was present between the PTFE insert and the NMR tube.

Ambient pressure measurements were made on a Bruker Avance spectrometer 500 MHz (11.7 T) with a power level attenuation of 7 dB, a pulse length of approximately 22 μs, 100 scans, and a relaxation time of 4.35 s ($t_1 \approx 0.87$ s) for samples with $NaNO_3$, 5.05 s ($t_1 \approx 1.01$ s) for samples with TMA nitrate, 5.41 s ($t_1 \approx 1.08$ s) for samples with

TEA nitrate, and 5.91 s ($t_1 \approx 1.18$ s) for samples with TBA nitrate were used. Shifts are reported against 85 % H_3PO_4 (aq) at 298 K. Temperatures (the Supporting Information, lists 1–4) are accurate to within 0.1 K. Samples were allowed to equilibrate for 10–20 min in the probe and were remeasured at room temperature throughout the experiment to ensure that changes in the spectra were reversible. All measurements were taken within a week of sample preparation.

High-pressure measurements were made on a sample with a $NaNO_3$ using home-built NMR probe[18] and a wide-bore Bruker Avance 400 MHz (9.4 T) spectrometer with a power level of attenuation 0 db, a pulse length of approximately 35 μs, 100 scans, and a relaxation time of 5.07 s ($t_1 \approx 1.01$ s). The sample was allowed to equilibrate after each pressure change (the Supporting Information, list 5) for 20–30 min.

Received: March 8, 2013
Revised: May 15, 2013
Published online: June 6, 2013

Keywords: actinides · environmental chemistry · geochemistry · kinetics · NMR spectroscopy

[1] a) P. C. Burns, K.-A. Kubatko, G. Sigmon, B. J. Fryer, J. E. Gagnon, M. R. Antonio, L. Soderholm, *Angew. Chem.* **2005**, *117*, 2173; *Angew. Chem. Int. Ed.* **2005**, *44*, 2135; b) G. E. Sigmon, D. K. Unruh, J. Ling, B. Weaver, M. Ward, L. Pressprich, A. Simonetti, P. C. Burns, *Angew. Chem.* **2009**, *121*, 2775; *Angew. Chem. Int. Ed.* **2009**, *48*, 2737.
[2] P. C. Burns, R. C. Ewing, A. Navrotsky, *Science* **2012**, *335*, 1184.
[3] M. Nyman, P. C. Burns, *Chem. Soc. Rev.* **2012**, *41*, 7354.
[4] a) A. Gil, D. Karhánek, P. Miró, M. R. Antonio, M. Nyman, C. Bo, *Chem. Eur. J.* **2012**, *18*, 8340; b) M. Nyman, M. A. Rodriguez, T. M. Alam, *Eur. J. Inorg. Chem.* **2011**, 2197.
[5] J. Ling, J. Qiu, G. E. Sigmon, M. Ward, J. E. S. Szymanowski, P. C. Burns, *J. Am. Chem. Soc.* **2010**, *132*, 13395.
[6] a) J. Jeener, B. H. Meier, P. Bachmann, R. R. Ernst, *J. Chem. Phys.* **1979**, *71*, 4546; b) G. Bodenhausen, H. Kogler, R. R. Ernst, *J. Magn. Reson.* **1984**, *58*, 370.
[7] F. Bloch, W. W. Hansen, M. Packard, *Phys. Rev.* **1946**, *70*, 474.
[8] H. M. McConnell, *J. Chem. Phys.* **1958**, *28*, 430.
[9] a) D. H. Aue, H. M. Webb, M. T. Bowers, *J. Am. Chem. Soc.* **1976**, *98*, 318; b) J. Palomo, P. N. Pintauro, *J. Membr. Sci.* **2003**, *215*, 103.
[10] B. Liedholm, M. Nilsson, *Acta Chem. Scand. Ser. B* **1988**, *42*, 289.
[11] J. F. Keggin, *Nature* **1933**, *131*, 908.
[12] a) J. J. Cowan, A. J. Bailey, R. A. Heintz, B. T. Do, K. I. Hardcastle, C. L. Hill, I. A. Weinstock, *Inorg. Chem.* **2001**, *40*, 6666; b) I. A. Weinstock, J. J. Cowan, E. M. G. Barbuzzi, H. Zeng, C. L. Hill, *J. Am. Chem. Soc.* **1999**, *121*, 4608.
[13] a) A. F. Wallace, G. V. Gibbs, P. M. Dove, *J. Phys. Chem. A* **2010**, *114*, 2534; b) L. J. Criscenti, J. D. Kubicki, S. L. Brantley, *J. Phys. Chem. A* **2006**, *110*, 198.
[14] P. M. Dove, N. Han, J. J. De Yoreo, *Proc. Natl. Acad. Sci. USA* **2005**, *102*, 15357.
[15] J. R. Rustad, W. H. Casey, *Nat. Mater.* **2012**, *11*, 223.
[16] a) E. M. Villa, C. A. Ohlin, J. R. Rustad, W. H. Casey, *J. Am. Chem. Soc.* **2010**, *132*, 5264; b) E. M. Villa, C. A. Ohlin, W. H. Casey, *Am. J. Sci.* **2010**, *310*, 629.
[17] E. M. Villa, C. A. Ohlin, W. H. Casey, *Chem. Eur. J.* **2010**, *16*, 8631.
[18] S. J. Harley, C. A. Ohlin, R. L. Johnson, A. F. Panasci, W. H. Casey, *Angew. Chem.* **2011**, *123*, 4559 – 4561; *Angew. Chem. Int. Ed.* **2011**, *50*, 4467 – 4469.

